ACS OMEGA

Open Access

http://pubs.acs.org/journal/acsodf

Article

Patterning Adhesive Layers for Array Electrodes via Electrochemically Grafted Polymers

Shuai Wen, Ruipeng Zhang, Yahui Zhao, Xinyue Xu, and Shaobo Ji*

Cite This: *ACS Omega* 2025, 10, 3190−3198

Read Online

ACCESS | Metrics & More | Article Recommendations | Supporting Information

ABSTRACT: Electrophysiological sensors (electrodes) are used to collect complex electrophysiological signals, providing extensive information about the body's condition. Reliable signal acquisition necessitates stable skin−electrode interfaces to prevent adverse effects arising from interface variations. Although the incorporation of conductive adhesive layers can improve the stability of these interfaces, in array electrodes, the layer may also cause short circuits and signal crosstalk. Here, we propose a general strategy for patterning the adhesive layer of array electrodes based on electrochemically grafted adhesive polymers (EGAPs). Utilizing the conductivity differences between the sensing sites and the substrate material of flexible electrodes, spatial selective loading of adhesive and ionically conductive polymers can be achieved through in situ electrochemical reactions, thus realizing spontaneous patterning. This EGAP-based method allows for a rapid and selective electrode surface modification in just two steps. Furthermore, array electrodes with EGAP acquired stable electrophysiological signals while improving the stability of the skin−electrode interface and the quality of signal collected and effectively avoided signal crosstalk between arrayed sensing sites.

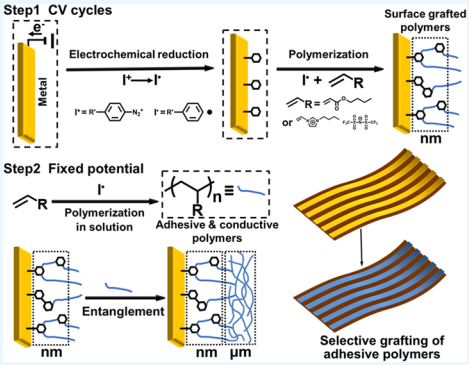

1. INTRODUCTION

Facing the significant challenge of global population aging and the urgent pursuit of healthy living, it is crucial to develop decentralized and personalized healthcare systems beyond traditional medicine. The realization of this goal relies on the development of portable, wearable healthcare devices based on flexible sensors.[1,2] In recent years, scientists have developed a variety of flexible sensors for detecting various physiological signals, including strain sensors (for detecting pulse, heartbeat, respiration, etc.),[3,4] temperature sensors,[5,6] optical sensors (for detecting blood pressure, etc.),[7,8] chemical sensors,[9,10] and electrophysiological sensors.[11−13] These sensors and flexible devices have different requirements for the skin−sensor interfaces.[14,15]

Among them, electrophysiological sensors (electrodes) are particularly special. They are used to collect complex electrophysiological signals, providing detailed and specific information about the biosystem, thus playing an important role in medical research, disease diagnosis, and human−machine interactions.[16−18] The complexity and richness of these signals impose higher demands on the skin−electrode interfaces: they must maintain intimate contact to avoid adverse effects caused by interface instability (e.g., gaps due to skin texture or interface detachment caused by bioliquids), which can lead to noise and signal loss.[19] To address this issue, conductive adhesive layers are usually introduced at the skin−electrode interfaces to establish intimate and stable signal transmission interfaces, such as adhesive hydrogels and polymers.[20−23]

With the increasing demand for electrode functionalization, patterned electrodes have garnered more attention.[24,25] For example, breathable electrodes are suitable for long-term monitoring, preventing sweat accumulation and enhancing long-term wearing comfortability.[26−28] Array electrodes not only provide abundant physiological information in electrophysiological monitoring but also can be combined with machine learning for human−machine interactions.[18,29−33] However, introducing continuous conductive adhesive layers to such patterned electrodes might hinder their functions, i.e., reducing the breathability by blocking the pores, or leading to short circuits between different subelectrodes and causing signal crosstalk in array electrodes.

Facing this problem of array electrodes, there were limited studies that provided certain solutions. Simply using tape or other adhesive materials to wrap the electrodes to the skin from the outside may not provide a secure fixation, especially when the skin undergoes significant deformations.[18,34] Thus, in a report, a gel to enhance the interfacial contact with the skin was manually added by dropping it on the surface of each sensing site of the array electrodes, which may not work well

Received: November 28, 2024
Revised: December 27, 2024
Accepted: January 9, 2025
Published: January 16, 2025

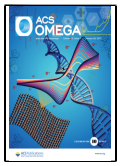

facing high-density and small-sized array electrodes.[35] It has also been reported that the modulation of adhesive layer conductivity could prevent the signal from attenuating at low conductivity and short-circuiting at high conductivity, which required optimization for different adhesive layers and was not a general method.[36] Although these methods allowed for electrode adhesion, they also had their limitations, especially from the perspective of convenience and universality. To solve this issue, it is necessary to find a simple method that can autonomously and selectively load adhesive layers.

In previous studies, fixed potential (FP) and cyclic voltammetry (CV) have been used for electrochemically controlled polymerization and grafting reactions at conductive surfaces.[37−40] Combined with the significant conductivity differences between the sensing sites and substrate materials of flexible electrodes, a theoretical basis for selective loading of the polymer adhesive layer is provided. Herein, spatial selective grafting of adhesive and ionic conductive polymers at the electrode sensing sites was achieved via controlled electrochemical polymerization. This method, based on electrochemically grafted adhesive polymers (EGAPs), required only two steps for swift and patterned adhesive layer loading. In EGAP, the butyl acrylate (BA) monomers provided adhesiveness, while the copolymerized ionic groups containing polymers provided sufficient conductivity. Array electrodes with EGAP demonstrated enhanced stability of the skin−electrode interfaces and were used to collect electrophysiological signals. They met the requirements for conforming to the human skin, providing adhesiveness and reusability, exhibiting skin interfacial impedance comparable to that of commercial gel electrodes, and effectively preventing signal crosstalk and short circuits. Our method is universal and facile for electrophysiological sensors. Employing this approach as a modification technique holds significant importance in reducing the cost and enhancing the performance of wearable health monitoring devices.

2. EXPERIMENTAL SECTION

2.1. Electrochemical Reaction Setup. As shown in Figure S1a, all reactions were carried out in a three-electrode electrochemical electrolytic cell. The working electrodes (WEs) were Cu sheets (99.9999% purity), Ti sheets (99.5% purity), or array electrodes (35 μm thick copper on polyimide (PI) film with desired patterns, customized from a PCB manufacturer: the substrate material for the electrodes was 100 μm thick PI films, a thin layer of copper (hundreds of nanometers, the manufacturer would not like to disclose the exact value) was first coated on the PI by thermal evaporation with masks of desired patterns, thus the array patterns were constructed. Then, the copper layer was thickened using electroplating to 35 μm, which would only deposit on the surface of the patterned copper surface). The counter electrode (CE) was a Pt wire electrode (purity of ≥99.99%). The reference electrode (RE) was a Ag/AgCl electrode.

2.2. Preparation of Electrolyte. In each case, all steps of solution formulation were performed in an electrolytic cell with a closed lid and inlet and outlet gas lines. *N*,*N*-Dimethylformamide (DMF, Ourchem) saturated with potassium chloride (KCl, Adamas) was used as the solvent. 0.1 mol/L of 1-ethyl-3-methylimidazolium tetrafluoroborate (ILB, Adamas, GR, 99%) or 1-ethyl-3-methylimidazolium bis(trifluoromepropyl sulfonyl)imide (ILN, Adamas, GR, >99%) was added to provide ionic conductivity of the electrolyte. BA (J&K Scientific) and 1-butyl-3-vinylimidazolium bis-((trifluorompropyl)sulfonyl)imide (M4, Adamas, GR, 99%) were added as monomers, and the total volume of monomers accounted for 50% of the total volume (50% vol) of the solution. Before the electrochemical reaction, the initiator was added to the mixed solution, with 4-bromobenzenediazonium tetrafluoroborate (BBD, Aladdin, AR, >97%) or 4-nitrobenzenediazonium tetrafluoroborate (NBD, Aladdin, BR, ≥98.0%) as initiators (Figure S1b). After solution preparation, oxygen was expelled by continuously purging N_2 through the cell (20 min), and then the gas lines were sealed to maintain a nitrogen environment in the cell. See the Supporting Information for detailed chemical selections (Table S1, Figures S2 and S3).

2.3. EGAP Modification on Electrodes. Electrochemical reactions were performed using an electrochemical workstation (model DH7000C, Donghua). Prescan (scan rate 0.1 V/s, vs RE) was performed under a nitrogen atmosphere to obtain the initiator's initiation characteristics and electrochemical curves (Figure S4). Based on the electrochemical curves, the range of reduction peak positions was determined, for which multiple cycles of low-rate scanning (scan rate 0.01 V/s, vs RE) were performed, and then, a suitable potential (corresponding to the position at which the reduction peaks ended) was selected for fixed potential (2 h, vs RE). At the end of the experiment, the working electrode was taken out, and the surface was rinsed (with ethanol or immersion) and dried to obtain the metal or array electrodes with EGAP. Generally, the process of EGAP modification of electrodes would about 3 h. First, it took about 10 min to prepare the electrolyte and set up the electrochemical device. Next, the creation of an inert atmosphere took 20 min. Then, cyclic voltammetry (CV cycling) would last for 15−30 min. The following process of fixing the reduction potential cost 2 h.

2.4. Copolymerization of Ionic Liquids and BA. In a sealed bottle, using DMF as the solvent, ionic liquids M1−M4 and BA were added in a molar ratio of 1:1. Trace amounts of AIBN were added as initiator, and the closed bottle was vented with nitrogen to exclude oxygen and stirred overnight at 60 °C. The product was then precipitated by ethyl ether. The resulting product was washed with ethyl ether and dried in a vacuum oven at 60 °C for 1 day to obtain the copolymer. The resulting polymers were uniformly coated with poly(dimethylsiloxane) (PDMS) for shear testing.

2.5. Morphology Characterization. For array electrodes with EGAP, the microscopic morphology of the adhesive layer on the metal surface was observed by using an optical microscope (model NI-SS, Nikon) and a scanning electron microscope (SEM, ZEISS G500).

2.6. Measurement of Mechanical and Electrical Properties. The mechanical properties were tested by a universal material testing machine (model YH-9002, Yuhong Optoelectronics) in tensile mode. Shear tests were conducted with EGAP-modified metal (Cu/Ti) bonded to PDMS at a shear rate of 60 mm/min. The impedance on the skin was measured by an electrochemical workstation (DH7000C, Donghua) with a range from 10 Hz to 10 kHz and an amplitude of 0.2 V RMS. The measurements were carried out by array electrodes with EGAP with a center distance of 1.6 cm between the two subelectrodes, and each subelectrode had a skin contact area of 0.2 cm^2. Commercial gel electrodes were also tested for comparison.

https://doi.org/10.1021/acsomega.4c10830
ACS Omega 2025, 10, 3190−3198

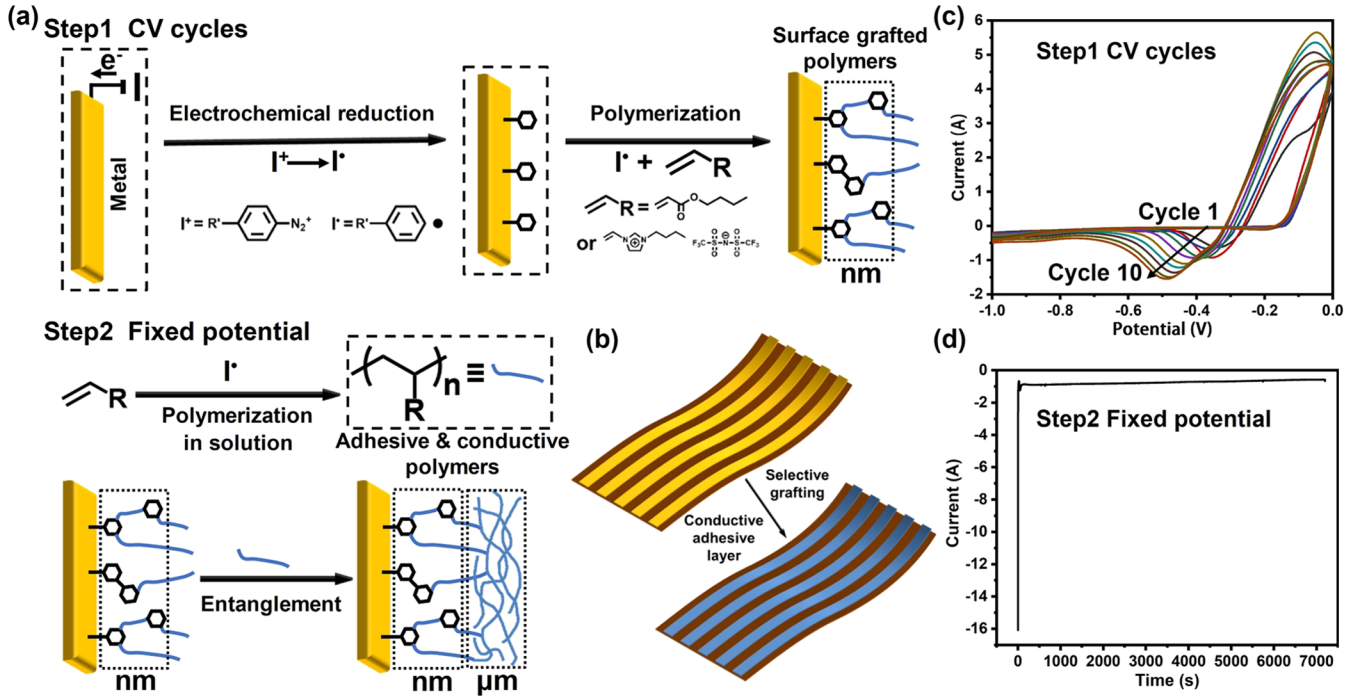

Figure 1. Schematic diagram and steps of EGAP modification. (a) Step 1: The phenyl radicals obtained by electrochemical reduction can react with metal and initiate the polymerization of monomers to generate grafted thin polymer layers. Step 2: The phenyl radicals initiate polymerization in the solution. The entanglement between grafted chains and free polymers enables the growth of the thicker adhesive layer. (b) Sensing sites of flexible electrodes have different electrical conductivities from that of the substrate. EGAP can be selectively loaded onto the sensing sites of the electrodes. (c) CV cycles and (d) fixed potential (FP) are the two steps of EGAP modification. During the first step, CV cycles, phenyl radicals are more involved in surface grafting to form a grafted layer. During the second step, FP, more polymers are generated and entangle with the grafted chains.

2.7. Recording of Electrophysiological Signals. The electrocardiogram (ECG) and electromyogram (EMG) signals were recorded with the Backyard Brains Spiker Box with three electrodes. Two signal-collecting electrodes were affixed to the human chest to detect ECG signals, and a reference electrode was affixed to the abdomen. Two signal-collecting electrodes were affixed to the forearm to detect EMG signals, and a reference electrode was affixed to the back of the hand on the same arm. Commercial gel electrodes or array electrodes modified by different methods were used.

3. RESULTS AND DISCUSSION

3.1. Design and Principle of EGAP. The sensing sites in flexible electrodes are mainly metals and carbon materials, which are conductive and can collect current. The electrode substrate materials are generally PI, PDMS, polyethylene terephthalate (PET), etc., which cannot conduct electrons. There is an obvious difference in conductivity between the two surfaces, providing the possibility to spatially selectively pattern the adhesive layer by electrochemical reactions. As shown in Figure 1a, using phenyl diazonium salt as an initiator, phenyl radicals could be generated by electrochemical reduction on the surface of the cathode. The radicals, on the one hand, could trigger the polymerization of adhesive and conductive monomers and, on the other hand, could bond onto metal surfaces to form grafted polymer chains. Chain entanglements would occur between the grafted polymer chains and chains polymerized in solution, which will make the grafted layer grow into an EGAP adhesive layer. Due to the high reactivity of the radicals, they could hardly diffuse to a long distance, so the grafting and polymerization could only occur near the conductive region of the electrode (within a nano-micrometers range), which can spontaneously realize the spatial selective patterning of the adhesive layer on the array electrode (Figure 1b). At the same time, the expected thickness (micrometers) of this adhesive layer will not affect the flexibility of the electrode itself.

The entire EGAP modification process required only two steps for patterning. The first step was CV cycles (Figure 1c), in which the phenyl radicals would bond with metal, and at the same time, the radicals would create initiation sites on the grafted groups by taking hydrogen atoms. A nanometer-thin layer of dendrite polymers was then grafted on the metal surface.[40,41] For this step, a prescan was performed to locate the potential range where the reduction peaks appeared (the reduction peaks corresponded to the reaction of phenyl radical production by phenyl diazonium salt reduction) before cycle 1 was performed. Then, low-rate CV cycles were carried out in the selected voltage range. In the latter cycles, the reduction peaks shifted to lower-voltage regions, which was caused by increased resistance from the grafted polymers. The second step is FP (Figure 1d), where the voltage at the end of the reduction peak in the last CV cycle (cycle 10) was chosen as the fixed reduction potential. In this step, the major reaction was the polymerization of the monomers in solution near the cathode. With a longer FP time, the current showed a decreasing trend, indicating an increased resistance caused by the grown polymers on the cathode surfaces. During FP polymerization, chain entanglement between the polymers in solution and the grafted chains led to a significantly increased thickness of the grafted polymer layer. With these two simple

https://doi.org/10.1021/acsomega.4c10830
ACS Omega 2025, 10, 3190−3198

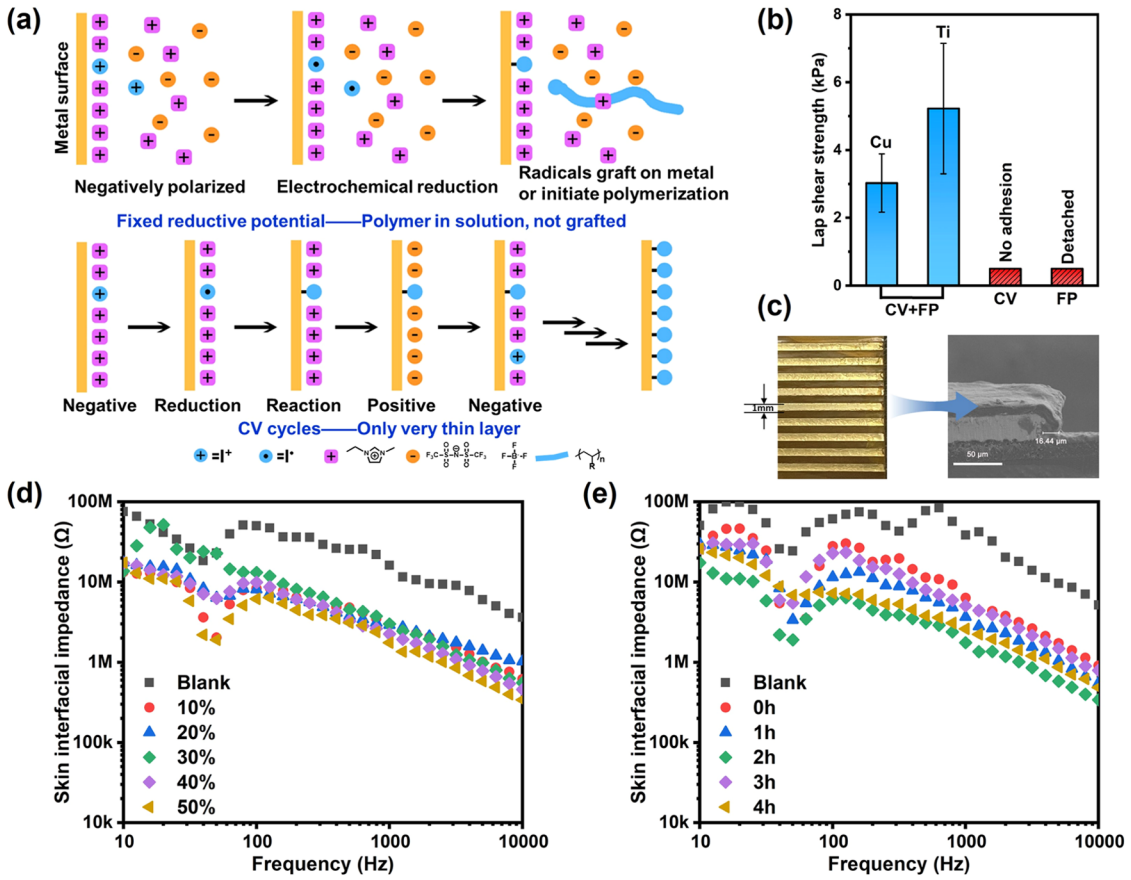

Figure 2. Loading of EGAP onto metal and array electrodes. (a) Possible mechanisms in the CV and FP steps. (b) Shear adhesion strength between PDMS and Cu/Ti sheets modified by CV, FP, and CV + FP. (c) Array electrode with EGAP and its microscopic morphology. (d) Skin interfacial impedance of EGAP-modified array electrode with different monomer (BA) contents in solution (10/20/30/40/50% vol). (e) Skin interfacial impedance of EGAP-modified array electrodes with different FP times (0/1/2/3/4 h). The distance between the arrayed electrode pairs used for measurement was 1.2 cm, and the contact area between the arrayed electrodes and the skin was approximately 0.2 cm^2 per electrode.

steps, micrometer-thick EGAP could be spatially selectively loaded on conductive sensing sites of array electrodes.

In the EGAPs, BA in the polymer chain acted as the backbone to provide adhesion; monomers containing ionic groups were copolymerized to provide ionic conductivity, making the layer suitable for signal transmission. EGAP improved the stability of the skin−electrode interfaces while ensuring signal acquisition quality. By optimization of the two-step electrochemical reaction conditions as well as the selected initiators, a balance between polymer chain growth and surface grafting could be achieved to enhance the quality of the adhesive layer. At the same time, after optimization of the monomer compositions, the skin interfacial impedance was lowered for electrophysiological signal acquisition with the priority of adhesion. Ultimately, the spontaneous patterning improved the adhesion of the array electrodes, while avoiding interference between different electrodes.

3.2. Loading of EGAP on Metals. The effective loading of EGAP could only be achieved when both steps had been involved, and the possible mechanism was speculated. Cu sheets, commonly used metals in electronics and sensors, were first tested for EGAP modification. For electrochemical reactions, three different procedures were conducted: (1) CV cycles only (CV), (2) fixed potential only (FP), and (3) CV cycles and fixed potential (CV + FP). As shown in Figure S5 and Supporting Video 1, the Cu sheet modified by CV had only a thin grafted layer on the surface exhibiting poor adhesion. The Cu sheet modified by FP hardly had a grafted layer; the polymer layer was shed in solution. The shape of this polymer layer confirmed that the highly active radicals could hardly diffuse over a long distance to initiate polymerization, which was the basis for spontaneous spatial selectivity. The Cu sheet modified by CV + FP had a clear adhesive layer on the surface. Similar results were achieved when using biocompatible Ti as substrate (Figures S6 and 2b). The above results indicated that the CV cycles were responsible for EGAP grafting, while FP triggered the growth of EGAP. Both steps were necessary for EGAP loading.

Possible mechanisms for the two steps were proposed (Figure 2a). During electrochemical reactions, double layers formed on the electrode surfaces. Here we focus on working electrodes, which were expected to be the cathode for EGAP modification. When FP was performed, the double layer was relatively static. Inactive cations competed with initiator cations to occupy the metal surface bilayer and might block most reactive sites (the molar ratio of inactive cation to initiator was approximately 1.35 in our case), which led to less involvement of diazonium radicals in surface grafting, and more polymerization occurred in the solution around the cathode. With little entanglement from grafted chains, the polymer can be dislodged in solution only eventually. While performing CV, the electrode flip occurred between every cycle, and the bilayer was relatively dynamic. More diazonium radicals could be adsorbed to the metal surface and participate

https://doi.org/10.1021/acsomega.4c10830
ACS Omega 2025, 10, 3190−3198

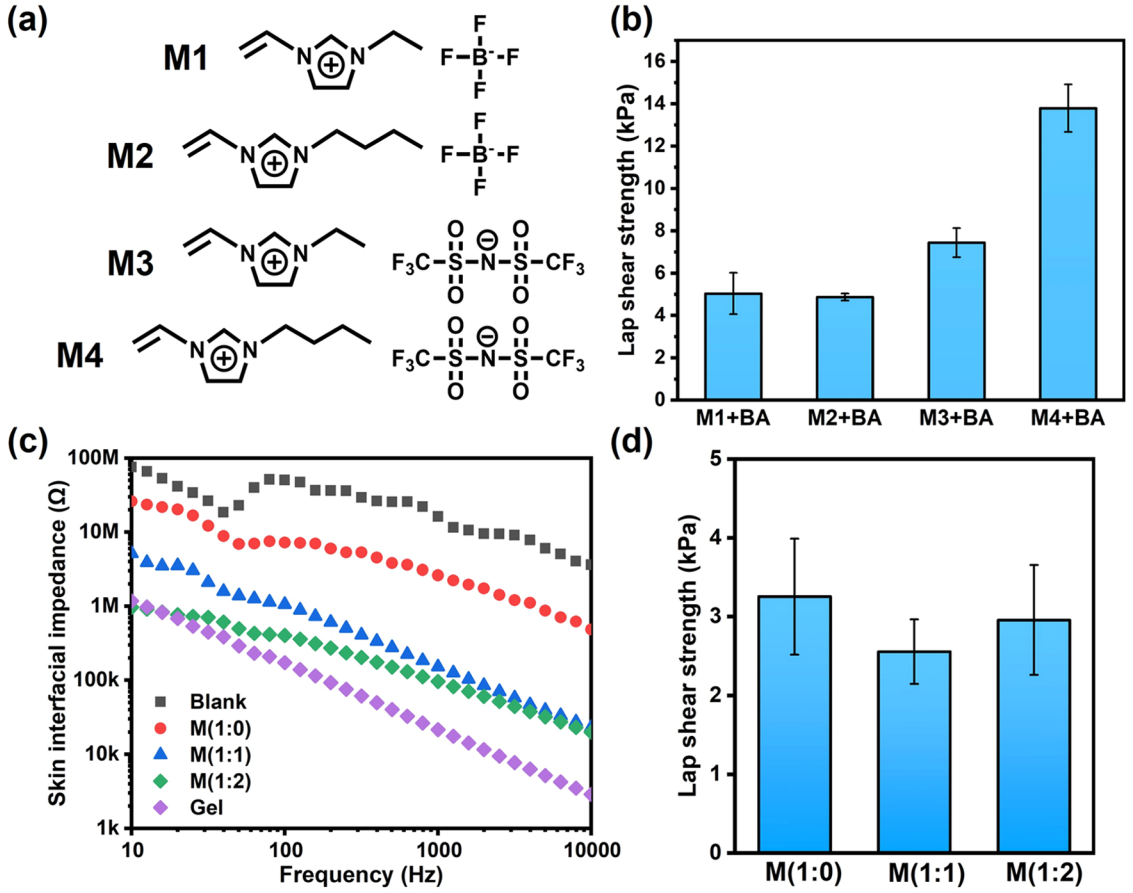

Figure 3. (a) Chemical structures of four vinyl-based ionic liquids (M1/M2/M3/M4). (b) Adhesion of the products after bulk polymerization of the four ionic liquids with BA (molar ratio 1:1). (c) Skin interfacial impedance of EGAP-modified array electrodes with different volume ratios of BA to M4, M (1:0), M (1:1), and M (1:2). The distance between the arrayed electrode pairs used for measurement was 1.2 cm, and the contact area between the arrayed electrodes and the skin was approximately 0.2 cm^2 per electrode. (d) Adhesion of EGAP-modified Cu sheets with different volume ratios of BA to M4, M (1:0), M (1:1), M (1:2).

in the grafting process, and a thin polymer layer with sufficient chains for entanglement was grown on the metal surface. In the 2-step modification, CV and FP were performed successively, and both surface grafting and molecular polymerization occurred. The presence of chain entanglements, in turn, allowed the grafted layer and the polymer layer to establish a linkage, realizing the effective loading of the adhesive layer.

It was also found that the EGAP modification had to be carried out in a sealed container to avoid quenching of radicals by O_2. The surface of the Cu sheet obtained by using EGAP modification in the open air was smooth, and no adhesive layer was obtained (Figure S7). The versatility of the method of metal modification using EGAP has enabled the effective loading of the adhesive layer on other metals, such as the highly biocompatible metal Ti. Under similar electrochemical conditions, the same loading results as those of Cu sheets were obtained for Ti (Figure S6).

To obtain stable electrophysiological signals, robust adhesion of the adhesive layer between the skin and the electrode is essential. To verify this, we performed shear tests using Cu sheets modified with EGAP. They were pressed together with skin-mimetic PDMS to assess the adhesion of EGAP. As shown in Figure 2b, the shear strength of the adhesive layer obtained from the Cu sheet modified by CV + FP is around 3 kPa, which satisfied the need for the electrodes to adhere to the skin. As discussed above, the Cu sheets modified by CV or FP were not adhesive and not able to be tested for a value. Meanwhile, EGAP-modified Ti sheets gave out the same results. The shear strength of the adhesive layer obtained from the Ti sheet modified with CV + FP was around 5.2 kPa. By the modification of these two metals, it was confirmed that the EGAP modification of the metals could provide an adhesive layer for on-skin electrodes.

3.3. Loading of EGAP on Array Electrodes and Impedance Optimization. Based on the conditions of metals, EGAP modification of array electrodes was carried out to achieve the patterning of the adhesive layers. Under scanning electron microscopy (SEM), it could be observed that the adhesive layer obtained by EGAP modification was grown only on the conductive region of the array electrode, and not on the flexible substrate PI. The adhesive layer had a thickness on the order of 10 μm (Figure 2c), and only exceeded the boundary of electrodes for less than 20 μm, indicating that this method was capable of patterning on dense patterns with high resolution and hundreds or even tens of micrometers gaps.

With other conditions constant, the array electrodes were modified with EGAP by modulating the time of fixation potential (0/1/2/3/4 h) and the content of the monomer (BA) in solution (10/20/30/40/50% vol). Skin interface impedance is essential for the detection of electrophysiological signals at the body surface; thus, it was characterized to select

https://doi.org/10.1021/acsomega.4c10830
ACS Omega 2025, 10, 3190−3198

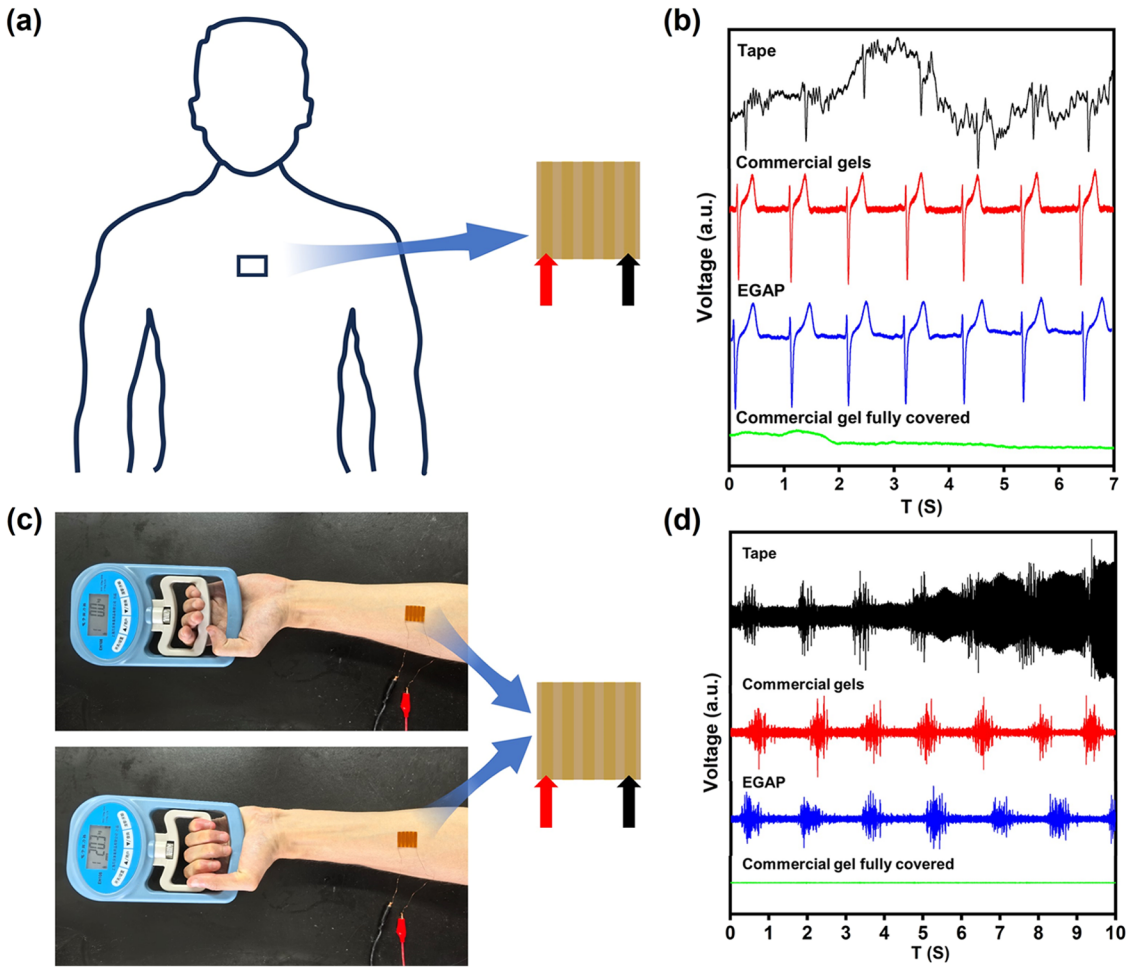

Figure 4. Electrophysiological detection by EGAP-modified array electrodes. (a) Illustration of the array position and electrode connection during the ECG test at the human chest. (b) ECG recorded by array electrodes under different conditions. (c) Illustration of the array position and electrode connection during the EMG test on the forearm using a grip. (d) EMG recorded by array electrodes under different conditions. The four signals in ECG and EMG correspond to array electrodes under the conditions (1) covered with adhesive tape externally for immobilization, (2) commercial gel dotted on the sensing sites of the electrodes, (3) EGAP-modified, and (4) fully coated with commercial gel, respectively.

the optimized condition. The lower the skin interfacial impedance, the better the contact between the skin and the electrodes and the better the accuracy of detection for electrophysiological signals. As shown in Figure 2d,e, it can be found that the lowest skin interfacial impedance corresponds to the following conditions: the time of fixation potential is 2 h, and the content of the monomer in the solution is 50% vol.

Even under optimal conditions, the skin interfacial impedance of the array electrodes modified by EGAP was much higher than that of commercially available gel electrodes (its impedance at 10 Hz was about 1 MΩ, and each electrode had a contact area of 0.785 cm^2 with the skin). This was due to the poor conductivity of the adhesive layer obtained with only BA as the monomer. Therefore, to solve this problem and reduce the skin interface impedance, ionic groups were introduced to the adhesive layer to establish ionic conductive channels between the electrode and the human skin to enhance the signaling ability. Four vinyl-based ionic liquids (M1/M2/M3/M4) were tested (Figure 3a). They were first thermally copolymerized with BA to compare the adhesiveness of the copolymers. The shear test results (Figure 3b) showed that the shear strength of M4 + BA was around 13.8 kPa, which had the best adhesion, and thus, M4 was selected as the ionic monomer to be introduced into the adhesive layer.

With the total content of the two monomers in the solution remaining at 50% vol of the electrolyte, the volume ratio of BA to M4 was varied to be M (1:0)/M (1:1)/M (1:2), where M (1:0) denotes that only BA was used as the monomer. Array electrodes were modified with EGAP using these monomer ratios, and their skin interfacial impedance was characterized. As shown in Figure 3c, the skin interfacial impedance of the array electrodes with EGAP of M (1:1) and M (1:2) was significantly reduced, which substantially enhanced the signaling ability. The array electrodes with EGAP of M (1:2) had an impedance comparable to that of commercial gel electrodes over a wide frequency range.

EGAP-modified Cu sheets were fabricated to test the adhesion of the above layers. As shown in Figure 3d, the adhesion of the Cu sheet with EGAP containing M4 had decreased a little compared to that of pure BA ones but did not exhibit an obvious difference. Therefore, the monomer ratio was chosen based on the skin interfacial impedance. Array electrodes with EGAP of M (1:2) were used for the detection of electrophysiological signals. The short circuit was also simulated by attaching a layer of commercial gels to the array covering multiple electrodes (Figure S8). The significantly

https://doi.org/10.1021/acsomega.4c10830
ACS Omega 2025, 10, 3190−3198

decreased impedance reflected the short circuit between different electrodes, which would lead to signal crosstalk. As a comparison, EGAP could be spatially selectively patterned on the sensing sites of array electrodes and effectively avoid signal crosstalk.

3.4. Electrophysiological Detection by Array Electrodes with EGAP. Electrocardiogram (ECG) reflects the activity of the human heart and is one of the most important electrophysiological signals. Array electrodes were attached to a human chest to collect ECG signals under different conditions. The attachment position and electrode connection are shown in Figure 4a. The ECG signals were collected continuously using (1) array electrodes fixed externally with tape, (2) array electrodes with commercial gel dots applied on the sensing sites, (3) array electrodes modified with EGAP, and (4) array electrodes fully coated with commercial gel for comparison. The array electrodes without modification could not intimately contact the chest and were highly susceptible to falling off and failing to acquire signals. As shown in Figure 4b, even if the electrodes were fixed with adhesive tape from the outside of the electrodes, the rise and fall of the chest during the measurement will cause the electrodes to loosen and signal drift. The ECG signals obtained from the array electrodes with EGAP were consistent with those with commercial gel dotted on the electrodes. The noise of the former signal in the baseline was lower than the latter one as the commercial gel had lower viscosity for the convenience of coating but also lower adhesion. The manual dapping of the gel would be time-consuming and laborious when used on a large scale. Moreover, during the process of dispensing gels and transferring electrodes, the gels on neighboring subelectrodes tend to connect, leading to short circuits between electrodes as well as signal interferences, as simulated here in case (4). The flexible nature of the PI-based array electrode guaranteed its function during and after deformation. The tiny resistance changes during bending (Figure S9a) ensured reliable signal acquisition on curved chest or arms. The EGAP modification would not be affected by the deformation of the electrodes. As shown in Figure S9b, the array electrodes still functioned well to collect stable and accurate ECG signals after 10 bending cycles.

In addition, array electrodes with EGAP could be used for stable collection of other electrophysiological signals, such as electromyography (EMG), for which the signal-to-noise ratio (SNR) could be calculated more easily for quantitative comparison. The same array electrode conditions (1), (2), (3), and (4) were used on forearms to collect EMG signals (Figures 4c and S10). Similar results to those for ECG were obtained (Figure 4d). The signal of the electrodes with tape deteriorated during muscle deformation, with an SNR of only 5.93 dB for even the initial stable section. The array electrodes coated with commercial gel dots corresponded to an SNR of 11.01 dB, and the array electrodes modified with EGAP corresponded to an SNR of 11.69 dB. These values further confirmed that the performance of the EGAP was comparable to that of the commercially available gels. In both ECG detection and EMG detection, the EGAP-modified array electrodes obtained stable electrophysiological signals and effectively avoided short circuits between electrodes as well as signal interferences, benefiting from the spontaneous patterning of EGAP on array electrodes.

The adhesive layers of the array electrodes with EGAP were stable and would not be affected by long-term storage or repeated usage. The array electrodes with EGAP stored for 3 months remained intact (Figure S11b), and ECG signals could still be acquired stably and accurately (Figure S12). In addition, after multiple testing with repeated attaching and detaching the electrodes from skin, the adhesive layer was retained on the surface of the electrodes and could still support stable ECG detections (Figures S11c and S13). Even if the adhesive layer might fail when accidentally damaged, the electrode surfaces could be easily regenerated by gentle cleaning (Supporting Video 2) and reloading of the adhesive layer after a second modification. The second modification resulted in an adhesive layer that was identical to that of the first modification (Figure S11d) and was also capable of stable and accurate ECG signal acquisition (Figure S14). These samples were fabricated from different patches, indicating good reproducibility of the patterning process.

4. CONCLUSIONS

In summary, a general method for patterning the adhesive layer on array electrodes based on electrochemically grafted polymers was demonstrated. This method required only two steps for the fast and selective modification of electrodes: CV cycles for grafting polymer chains on conductive surfaces, FP for polymerizing monomers around the conductive sites; the entanglement between surface grafted chains with polymers in solution resulted in the micrometer-thick EGAP layer. By controlling the electrochemical reaction conditions, initiators, and monomers, we optimized the adhesion and ionic conductivity of EGAP were optimized. EGAP-modified array electrodes had improved adhesion with skin interfacial impedance comparable to that of commercial gel electrodes. The ECG and EMG collected by them also exhibited qualities comparable to those of commercial gels and avoided signal crosstalk. This method also showed some versatility, as it applied to both the commonly used metal Cu and the highly biocompatible metal Ti. For wearable electrophysiological sensors, our method enables the spontaneous patterning of adhesive layers on arrayed electrodes and can be reused, which is promising for reducing the cost and improving the performance of flexible electrodes. In the future, its application is expected to expand to more complex electrode systems, such as stretchable ones, microelectrode arrays, and breathable electrodes, as a universal patterning strategy.

■ ASSOCIATED CONTENT

Supporting Information

The Supporting Information is available free of charge at https://pubs.acs.org/doi/10.1021/acsomega.4c10830.

Selection of initiator compositions (Figures S1−S12) (PDF)

Adhesiveness of modified Cu sheets with different procedures (MP4)

Gentle cleaning of adhesive layer from electrode surfaces for EGAP regeneration (MP4)

■ AUTHOR INFORMATION

Corresponding Author

Shaobo Ji − *Institute of Functional Nano & Soft Materials (FUNSOM), College of Nano Science and Technology (CNST), Jiangsu Key Laboratory for Carbon-Based Functional Materials & Devices, Soochow University, Suzhou*

https://doi.org/10.1021/acsomega.4c10830
ACS Omega 2025, 10, 3190−3198

215123, China; orcid.org/0000-0002-6333-3561; Email: sbji@suda.edu.cn

Authors

Shuai Wen − *Institute of Functional Nano & Soft Materials (FUNSOM), College of Nano Science and Technology (CNST), Jiangsu Key Laboratory for Carbon-Based Functional Materials & Devices, Soochow University, Suzhou 215123, China*

Ruipeng Zhang − *Institute of Functional Nano & Soft Materials (FUNSOM), College of Nano Science and Technology (CNST), Jiangsu Key Laboratory for Carbon-Based Functional Materials & Devices, Soochow University, Suzhou 215123, China*

Yahui Zhao − *Institute of Functional Nano & Soft Materials (FUNSOM), College of Nano Science and Technology (CNST), Jiangsu Key Laboratory for Carbon-Based Functional Materials & Devices, Soochow University, Suzhou 215123, China*

Xinyue Xu − *Department of Polymer Science and Engineering, College of Chemistry, Chemical Engineering and Materials Science, Soochow University, Suzhou 215123, China*

Complete contact information is available at: https://pubs.acs.org/10.1021/acsomega.4c10830

Notes

The authors declare no competing financial interest.

■ ACKNOWLEDGMENTS

This work was supported by the Collaborative Innovation Center of Suzhou Nano Science and Technology, Suzhou Key Laboratory of Surface and Interface Intelligent Matter (Grant No. SZS2022011), the Gusu Innovation and Entrepreneurship Talent Program−Major Innovation Team (ZXD2023002), Natural Science Foundation of Basic Research Program of Jiangsu Province (BK20240826), and National Natural Science Foundation of China (52473218).

■ REFERENCES

(1) Luo, Y.; Abidian, M. R.; Ahn, J. H.; Akinwande, D.; Andrews, A. M.; Antonietti, M.; Bao, Z.; Berggren, M.; Berkey, C. A.; Bettinger, C. J.; Chen, J.; Chen, P.; Cheng, W.; Cheng, X.; Choi, S. J.; Chortos, A.; Dagdeviren, C.; Dauskardt, R. H.; Di, C. A.; Dickey, M. D.; Duan, X.; Facchetti, A.; Fan, Z.; Fang, Y.; Feng, J.; Feng, X.; Gao, H.; Gao, W.; Gong, X.; Guo, C. F.; Guo, X.; Hartel, M. C.; He, Z.; Ho, J. S.; Hu, Y.; Huang, Q.; Huang, Y.; Huo, F.; Hussain, M. M.; Javey, A.; Jeong, U.; Jiang, C.; Jiang, X.; Kang, J.; Karnaushenko, D.; Khademhosseini, A.; Kim, D. H.; Kim, I. D.; Kireev, D.; Kong, L.; Lee, C.; Lee, N. E.; Lee, P. S.; Lee, T. W.; Li, F.; Li, J.; Liang, C.; Lim, C. T.; Lin, Y.; Lipomi, D. J.; Liu, J.; Liu, K.; Liu, N.; Liu, R.; Liu, Y.; Liu, Y.; Liu, Z.; Liu, Z.; Loh, X. J.; Lu, N.; Lv, Z.; Magdassi, S.; Malliaras, G. G.; Matsuhisa, N.; Nathan, A.; Niu, S.; Pan, J.; Pang, C.; Pei, Q.; Peng, H.; Qi, D.; Ren, H.; Rogers, J. A.; Rowe, A.; Schmidt, O. G.; Sekitani, T.; Seo, D. G.; Shen, G.; Sheng, X.; Shi, Q.; Someya, T.; Song, Y.; Stavrinidou, E.; Su, M.; Sun, X.; Takei, K.; Tao, X. M.; Tee, B. C. K.; Thean, A. V. Y.; Trung, T. Q.; Wan, C.; Wang, H.; Wang, J.; Wang, M.; Wang, S.; Wang, T.; Wang, Z. L.; Weiss, P. S.; Wen, H.; Xu, S.; Xu, T.; Yan, H.; Yan, X.; Yang, H.; Yang, L.; Yang, S.; Yin, L.; Yu, C.; Yu, G.; Yu, J.; Yu, S. H.; Yu, X.; Zamburg, E.; Zhang, H.; Zhang, X.; Zhang, X.; Zhang, X.; Zhang, Y.; Zhang, Y.; Zhao, S.; Zhao, X.; Zheng, Y.; Zheng, Y. Q.; Zheng, Z.; Zhou, T.; Zhu, B.; Zhu, M.; Zhu, R.; Zhu, Y.; Zhu, Y.; Zou, G.; Chen, X. Technology Roadmap for Flexible Sensors. *ACS Nano* **2023**, *17* (6), 5211−5295.

(2) Gao, W.; Ota, H.; Kiriya, D.; Takei, K.; Javey, A. Flexible Electronics toward Wearable Sensing. *Acc. Chem. Res.* **2019**, *52* (3), 523−533.

(3) Ni, Q. Y.; He, X. F.; Zhou, J. L.; Yang, Y. Q.; Zeng, Z. F.; Mao, P.; Luo, Y. H.; Xu, J. M.; Jiang, B.; Wu, Q.; Wang, B.; Qin, Y. Q.; Gong, L. X.; Tang, L. C.; Li, S. N. Mechanical tough and stretchable quaternized cellulose nanofibrils/MXene conductive hydrogel for flexible strain sensor with multi-scale monitoring. *J. Mater. Sci. Technol.* **2024**, *191*, 181−191.

(4) Li, J.; Yao, Z.; Meng, X.; Zhang, X.; Wang, Z.; Wang, J.; Ma, G.; Liu, L.; Zhang, J.; Niu, S.; Han, Z.; Ren, L. High-Fidelity, Low-Hysteresis Bionic Flexible Strain Sensors for Soft Machines. *ACS Nano* **2024**, *18* (3), 2520−2530.

(5) Zhang, J.; Yan, K.; Huang, J.; Sun, X.; Li, J.; Cheng, Y.; Sun, Y.; Shi, Y.; Pan, L. Mechanically Robust, Flexible, Fast Responding Temperature Sensor and High-Resolution Array with Ionically Conductive Double Cross-Linked Hydrogel. *Adv. Funct. Mater.* **2024**, *34* (21), No. 2314433.

(6) Yao, P.; Bao, Q.; Yao, Y.; Xiao, M.; Xu, Z.; Yang, J.; Liu, W. Environmentally Stable, Robust, Adhesive, and Conductive Supramolecular Deep Eutectic Gels as Ultrasensitive Flexible Temperature Sensor. *Adv. Mater.* **2023**, *35* (21), No. 2300114.

(7) Wang, Z.; Chen, Z.; Ma, L.; Wang, Q.; Wang, H.; Leal-Junior, A.; Li, X.; Marques, C.; Min, R. Optical Microfiber Intelligent Sensor: Wearable Cardiorespiratory and Behavior Monitoring with a Flexible Wave-Shaped Polymer Optical Microfiber. *ACS Appl. Mater. Interfaces* **2024**, *16* (7), 8333−8345.

(8) Chang, S.; Koo, J. H.; Yoo, J.; Kim, M. S.; Choi, M. K.; Kim, D. H.; Song, Y. M. Flexible and Stretchable Light-Emitting Diodes and Photodetectors for Human-Centric Optoelectronics. *Chem. Rev.* **2024**, *124* (3), 768−859.

(9) Hu, C.; Wang, L.; Liu, S.; Sheng, X.; Yin, L. Recent Development of Implantable Chemical Sensors Utilizing Flexible and Biodegradable Materials for Biomedical Applications. *ACS Nano* **2024**, *18* (5), 3969−3995.

(10) Gao, F.; Liu, C.; Zhang, L.; Liu, T.; Wang, Z.; Song, Z.; Cai, H.; Fang, Z.; Chen, J.; Wang, J.; Han, M.; Wang, J.; Lin, K.; Wang, R.; Li, M.; Mei, Q.; Ma, X.; Liang, S.; Gou, G.; Xue, N. Wearable and flexible electrochemical sensors for sweat analysis: a review. *Microsyst. Nanoeng.* **2023**, *9* (1), No. 1.

(11) Ma, Y.; Zhang, Y.; Cai, S.; Han, Z.; Liu, X.; Wang, F.; Cao, Y.; Wang, Z.; Li, H.; Chen, Y.; Feng, X. Flexible Hybrid Electronics for Digital Healthcare. *Adv. Mater.* **2020**, *32* (15), No. e1902062.

(12) Lim, H. R.; Kim, H. S.; Qazi, R.; Kwon, Y. T.; Jeong, J. W.; Yeo, W. H. Advanced Soft Materials, Sensor Integrations, and Applications of Wearable Flexible Hybrid Electronics in Healthcare, Energy, and Environment. *Adv. Mater.* **2020**, *32* (15), No. e1901924.

(13) Wang, J.; Wang, C.; Cai, P.; Luo, Y.; Cui, Z.; Loh, X. J.; Chen, X. Artificial Sense Technology: Emulating and Extending Biological Senses. *ACS Nano* **2021**, *15* (12), 18671−18678.

(14) Kim, D. W.; Kong, M.; Jeong, U. Interface Design for Stretchable Electronic Devices. *Adv. Sci.* **2021**, *8* (8), No. 2004170.

(15) Li, S.; Lan, Y.; Huang, Y.; Chen, Y.; Su, Y. A Universal Size Design Principle for Stretchable Inorganic Electronics to Work Consistently under Different Interface Conditions. *Adv. Funct. Mater.* **2023**, *33* (7), No. 2210880.

(16) Wu, H.; Yang, G.; Zhu, K.; Liu, S.; Guo, W.; Jiang, Z.; Li, Z. Materials, Devices, and Systems of On-Skin Electrodes for Electrophysiological Monitoring and Human-Machine Interfaces. *Adv. Sci.* **2021**, *8* (2), No. 2001938.

(17) Zhang, Z.; Yang, J.; Wang, H.; Wang, C.; Gu, Y.; Xu, Y.; Lee, S.; Yokota, T.; Haick, H.; Someya, T.; Wang, Y. A 10-micrometer-thick nanomesh-reinforced gas-permeable hydrogel skin sensor for long-term electrophysiological monitoring. *Sci. Adv.* **2024**, *10* (2), No. eadj5389.

(18) Moin, A.; Zhou, A.; Rahimi, A.; Menon, A.; Benatti, S.; Alexandrov, G.; Tamakloe, S.; Ting, J.; Yamamoto, N.; Khan, Y.; Burghardt, F.; Benini, L.; Arias, A. C.; Rabaey, J. M. A wearable

biosensing system with in-sensor adaptive machine learning for hand gesture recognition. *Nat. Electron.* **2021**, *4* (1), 54−63.
(19) Yang, H.; Ji, S.; Chaturvedi, I.; Xia, H.; Wang, T.; Chen, G.; Pan, L.; Wan, C.; Qi, D.; Ong, Y. S.; Chen, X. Adhesive Biocomposite Electrodes on Sweaty Skin for Long-Term Continuous Electrophysiological Monitoring. *ACS Mater. Lett.* **2020**, *2* (5), 478−484.
(20) Ma, Z.; Bao, G.; Li, J. Multifaceted Design and Emerging Applications of Tissue Adhesives. *Adv. Mater.* **2021**, *33* (24), No. 2007663.
(21) Nam, S.; Mooney, D. Polymeric Tissue Adhesives. *Chem. Rev.* **2021**, *121* (18), 11336−11384.
(22) Yuk, H.; Varela, C. E.; Nabzdyk, C. S.; Mao, X.; Padera, R. F.; Roche, E. T.; Zhao, X. Dry double-sided tape for adhesion of wet tissues and devices. *Nature* **2019**, *575* (7781), 169−174.
(23) Ji, S.; Wan, C.; Wang, T.; Li, Q.; Chen, G.; Wang, J.; Liu, Z.; Yang, H.; Liu, X.; Chen, X. Water-Resistant Conformal Hybrid Electrodes for Aquatic Endurable Electrocardiographic Monitoring. *Adv. Mater.* **2020**, *32* (26), No. 2001496.
(24) Choi, H.; Luo, Y.; Olson, G.; Won, P.; Shin, J. H.; Ok, J.; Yang, Y. J.; Kim, T. I.; Majidi, C. Highly Stretchable and Strain-Insensitive Liquid Metal based Elastic Kirigami Electrodes (LM-eKE). *Adv. Funct. Mater.* **2023**, *33* (30), No. 2301388.
(25) Park, S.; Ban, S.; Zavanelli, N.; Bunn, A. E.; Kwon, S.; Lim, H. R.; Yeo, W. H.; Kim, J. H. Fully Screen-Printed PI/PEG Blends Enabled Patternable Electrodes for Scalable Manufacturing of Skin-Conformal, Stretchable, Wearable Electronics. *ACS Appl. Mater. Interfaces* **2023**, *15* (1), 2092−2103.
(26) Zhang, B.; Li, J.; Zhou, J.; Chow, L.; Zhao, G.; Huang, Y.; Ma, Z.; Zhang, Q.; Yang, Y.; Yiu, C. K.; Li, J.; Chun, F.; Huang, X.; Gao, Y.; Wu, P.; Jia, S.; Li, H.; Li, D.; Liu, Y.; Yao, K.; Shi, R.; Chen, Z.; Khoo, B. L.; Yang, W.; Wang, F.; Zheng, Z.; Wang, Z.; Yu, X. A three-dimensional liquid diode for soft, integrated permeable electronics. *Nature* **2024**, *628* (8006), 84−92.
(27) Li, H.; Wang, Z.; Sun, M.; Zhu, H.; Liu, H.; Tang, C. Y.; Xu, L. Breathable and Skin-Conformal Electronics with Hybrid Integration of Microfabricated Multifunctional Sensors and Kirigami-Structured Nanofibrous Substrates. *Adv. Funct. Mater.* **2022**, *32* (32), No. 2202792.
(28) Li, Q.; Chen, G.; Cui, Y.; Ji, S.; Liu, Z.; Wan, C.; Liu, Y.; Lu, Y.; Wang, C.; Zhang, N.; Cheng, Y.; Zhang, K. Q.; Chen, X. Highly Thermal-Wet Comfortable and Conformal Silk-Based Electrodes for On-Skin Sensors with Sweat Tolerance. *ACS Nano* **2021**, *15* (6), 9955−9966.
(29) Zhao, X. F.; Yang, S. Q.; Wen, X. H.; Huang, Q. W.; Qiu, P. F.; Wei, T. R.; Zhang, H.; Wang, J. C.; Zhang, D. W.; Shi, X.; Lu, H. L. A Fully Flexible Intelligent Thermal Touch Panel Based on Intrinsically Plastic Ag2S Semiconductor. *Adv. Mater.* **2022**, *34* (13), No. 2107479.
(30) Zhou, Z.; Chen, K.; Li, X.; Zhang, S.; Wu, Y.; Zhou, Y.; Meng, K.; Sun, C.; He, Q.; Fan, W.; Fan, E.; Lin, Z.; Tan, X.; Deng, W.; Yang, J.; Chen, J. Sign-to-speech translation using machine-learning-assisted stretchable sensor arrays. *Nat. Electron.* **2020**, *3* (9), 571−578.
(31) Wang, S.; Nie, Y.; Zhu, H.; Xu, Y.; Cao, S.; Zhang, J.; Li, Y.; Wang, J.; Ning, X.; Kong, D. Intrinsically stretchable electronics with ultrahigh deformability to monitor dynamically moving organs. *Sci. Adv.* **2022**, *8* (13), No. eabl5511.
(32) Zheng, S.; Wang, X.; Li, W.; Liu, Z.; Li, Q.; Yan, F. Pressure-stamped stretchable electronics using a nanofibre membrane containing semi-embedded liquid metal particles. *Nat. Electron.* **2024**, *7* (7), 576−585.
(33) Wang, X.; Qiu, W.; Lu, C.; Jiang, Z.; Hou, C.; Li, Y.; Wang, Y.; Du, H.; Zhou, J.; Liu, X. Y. Fabrication of Flexible and Conductive Microneedle Array Electrodes from Silk Fibroin by Mesoscopic Engineering. *Adv. Funct. Mater.* **2024**, *34* (30), No. 2311535.
(34) Liu, J.; Zhang, X.; Liu, Y.; Rodrigo, M.; Loftus, P. D.; Aparicio-Valenzuela, J.; Zheng, J.; Pong, T.; Cyr, K. J.; Babakhanian, M.; Hasi, J.; Li, J.; Jiang, Y.; Kenney, C. J.; Wang, P. J.; Lee, A. M.; Bao, Z. Intrinsically stretchable electrode array enabled in vivo electrophysiological mapping of atrial fibrillation at cellular resolution. *Proc. Natl. Acad. Sci. U.S.A.* **2020**, *117* (26), 14769−14778.
(35) Yang, Q.; Wei, T.; Yin, R. T.; Wu, M.; Xu, Y.; Koo, J.; Choi, Y. S.; Xie, Z.; Chen, S. W.; Kandela, I.; Yao, S.; Deng, Y.; Avila, R.; Liu, T. L.; Bai, W.; Yang, Y.; Han, M.; Zhang, Q.; Haney, C. R.; Benjamin Lee, K.; Aras, K.; Wang, T.; Seo, M. H.; Luan, H.; Lee, S. M.; Brikha, A.; Ghoreishi-Haack, N.; Tran, L.; Stepien, I.; Aird, F.; Waters, E. A.; Yu, X.; Banks, A.; Trachiotis, G. D.; Torkelson, J. M.; Huang, Y.; Kozorovitskiy, Y.; Efimov, I. R.; Rogers, J. A. Photocurable bioresorbable adhesives as functional interfaces between flexible bioelectronic devices and soft biological tissues. *Nat. Mater.* **2021**, *20* (11), 1559−1570.
(36) Tria, M. C. R.; Grande, C. D.; Ponnapati, R. R.; Advincula, R. C. Electrochemical deposition and surface-initiated RAFT polymerization: protein and cell-resistant PPEGMEMA polymer brushes. *Biomacromolecules* **2010**, *11* (12), 3422−3431.
(37) Wang, Y.; Fantin, M.; Park, S.; Gottlieb, E.; Fu, L.; Matyjaszewski, K. Electrochemically Mediated Reversible Addition-Fragmentation Chain-Transfer Polymerization. *Macromolecules* **2017**, *50* (20), 7872−7879.
(38) Grande, C. D.; Tria, M. C. R.; Jiang, G.; Ponnapati, R. R.; Advíncula, R. C. Surface-Grafted Polymers from Electropolymerized Polythiophene RAFT Agent. *Macromolecules* **2011**, *44* (4), 966−975.
(39) Magenau, A. J. D.; Strandwitz, N. C.; Gennaro, A.; Matyjaszewski, K. Electrochemically Mediated Atom Transfer Radical Polymerization. *Science* **2011**, *332* (6025), 81−84.
(40) Tessier, L.; Deniau, G.; Charleux, B.; Palacin, S. Surface Electroinitiated Emulsion Polymerization (SEEP): A Mechanistic Approach. *Chem. Mater.* **2009**, *21* (18), 4261−4274.
(41) Deniau, G.; Azoulay, L.; Bougerolles, L.; Palacin, S. Surface Electroinitiated Emulsion Polymerization: grafted organic coatings from aqueous solutions. *Chem. Mater.* **2006**, *18* (23), 5421−5428.

https://doi.org/10.1021/acsomega.4c10830
ACS Omega 2025, 10, 3190−3198